Chapter-6

Application of Alicyclic Auxochrome in Synthesis of Glutathione-Detecting Ratiometric Fluorescent Probe

6. Application of Alicyclic Auxochrome in Synthesis of Glutathione-Detecting Ratiometric Fluorescent Probe

6.1. Background and Rationale

In the previous two chapters, we unequivocally demonstrated that cyclobutylaminated fluorophores, specifically coumarins, naphthalimides, and nitrobenzoxadiazole, possess higher quantum yields, superior photostability, excellent biocompatibility, and substantial cell permeability. Furthermore, the cyclobutylamine auxochrome boasts an inherent nitrogen centre that can be effectively employed for additional chemical functionalization, particularly with a response unit for detecting biomolecules and biochemicals indicative of disease biomarkers. In this chapter, we will demonstrate the effective application of cyclobutylaminated naphthalimide in designing and synthesizing a fluorescent probe, as we have planned from the outset.

Glutathione (GSH) is a crucial component of the reactive sulfur or thiol family, serving multiple physiological functions such as regulating oxidative stress, immune responses, detoxification, and gene expression.[1–3] GSH primarily functions in safeguarding cellular components against oxidative damage, facilitated by the enzymatic activity of GSH peroxidase (GPx). GSH undergoes a reduction in the presence of NADPH through the catalytic action of GSH reductase. Subsequently, GSH disulfide (GSSG) is formed through the oxidation of two reduced GSH molecules by GPx, leading to the reduction of hydrogen peroxide (H_2O_2) to water and molecular oxygen via a redox cycle, contributing to the maintenance of cellular homeostasis.[4–6] Moreover, GSH's reducing property allows for the conjugation with toxic reactive metabolites of xenobiotics, aiding in their elimination from the body. Dysregulation of GSH levels has been associated with various physiological conditions including AIDS, leukopenia, neurodegenerative diseases, cancer, HIV, liver injury, and other ailments.[7–14]

Consequently, the development of effective tools and methodologies for the selective and sensitive detection of GSH is paramount for early clinical diagnosis and preliminary research.

While a variety of sophisticated instruments such as mass spectrometry (MS), high-performance liquid chromatography (HPLC), HPLC-MS/MS, and capillary electrophoresis have been utilized for GSH detection and quantification, recent attention has turned toward fluorescence-based analytical techniques as a noninvasive, high-resolution, real-time monitoring tool for living systems. Despite numerous fluorescent probes developed for GSH monitoring, they often lack optimal photophysical and physicochemical properties due to presence of subpar fluorophores.

Hence, we sought to present the application of our cyclobutylaminated fluorophore in designing a novel fluorescent probe for effective GSH detection. We have synthesized a ratiometric fluorescent probe, **NAPB**, which comprises cyclobutylaminated naphthalimide (NCB) as the primary fluorophore, connected to a chloroacetyl unit for GSH recognition (figure 6.1). This recognition is facilitated by the nucleophilicity of thiols, allowing for a simple SN_2 nucleophilic substitution with the chlorine atom of the acetyl moiety. This is followed by a nucleophilic attack of the free amino group of GSH on the carbonyl of the response unit, resulting in the dissociation and release of the parent fluorophore. Post-synthesis of **NAPB**, our objective was to evaluate its sensitivity and selectivity to GSH and explore its potential applications for imaging GSH in living cells.

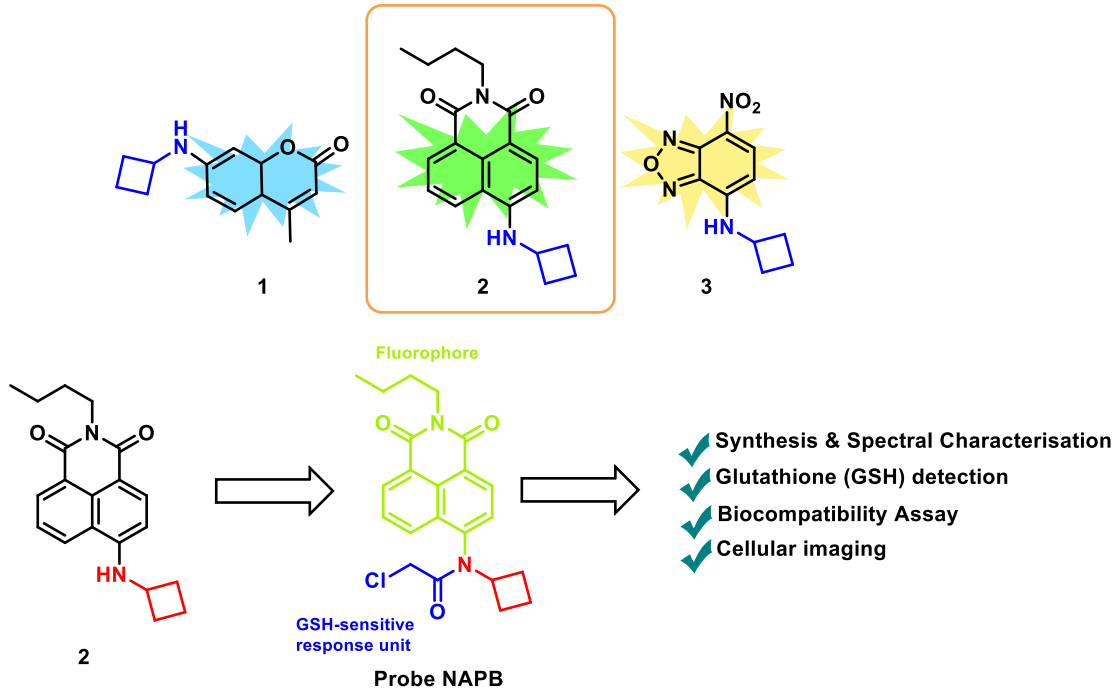

Figure 6.1. Illustration of application of cyclobutylaminated naphthalimide in designing a fluorescent probe **NAPB** for effective detection of GSH.

6.2. Results and Discussion

6.2.1. Synthesis of probe NAPB

Commercially available precursor 4-bromo-1,8-naphthalic anhydride (**A**) was refluxed with *n*-butyl-amine in ethanol for 2 h to yield intermediate **B** in 75 %. Intermediate **B** then undergoes aromatic substitution with cyclobutylamine in the presence of triethylamine (Et_3N) as base and dimethylsulfoxide (DMSO) as solvent for 6 h to afford **NCB** in 78 % yield. After its synthesis, **NCB** was subjected to simple nucleophilic substitution with 2-chloroacetyl chloride in the presence of a strong base under reflux conditions within a short period of 2 h to afford the probe **NAPB** in moderate yields of 76% (scheme 6.1). The chemical structure of the new target molecule was well characterized by standard spectroscopic techniques such as NMR and MS spectroscopies (see Appendix).

Scheme 6.1. Synthesis of NAPB from NCB.

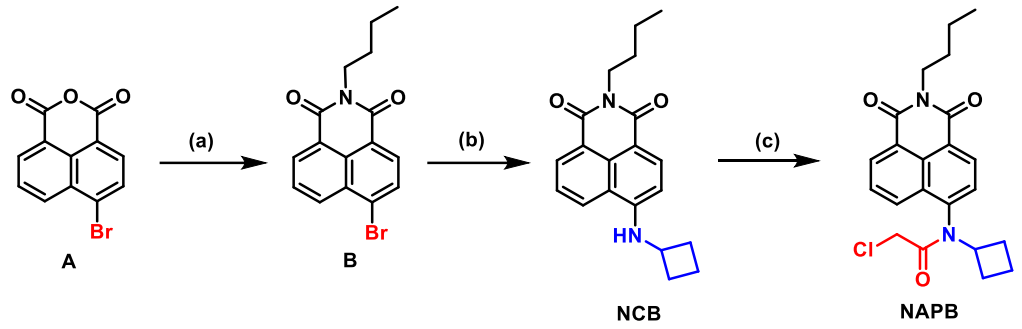

[a]**Reagents and conditions**: (a) **A** (3 mmol), *n*-butylamine (1.5 equiv.), EtOH (5 mL), refluxed at 80 °C for 2h, 75%; (b) **B** (0.3 mmol), triethylamine (1.5 equiv.) and cyclobutylamine (1.5 equiv.), DMSO (2 mL), heated at 110 °C for 6 h, 78%; (c) **NCB** (0.5 mmol), chloroacetyl chloride (5 eq.), dried Na_2CO_3 (2 eq.), ACN (3 mL), refluxed at 80 °C for 2h, 76%.

6.2.2. Sensing Mechanism and Selectivity of probe NAPB to GSH

We subjected **NAPB** (1.25 μM) to an equimolar amount of GSH in slightly basic conditions (pH 8.5) and ambient temperature. Within 5-10 minutes, a change of blue fluorescence to greenish-yellow fluorescence was observed in thin layer chromatogram (TLC) under UV light irradiation (λ_{ex}: 365 nm). After 30 mins, LC-MS analysis of the reaction mixture of **NAPB** and GSH was performed. The results indicated the complete disappearance of **NAPB** (m/z for $M+H^+$: 399.1681, 401.1819) and formation of **NCB** (m/z for $M+H^+$: 323.1933) along with a corresponding cyclization product for GSH (**GA**) (m/z for $M+H^+$: 348.8954) (**Scheme 6.2a**) (see Appendix). A similar observation was made when **NAPB** was subjected to an equimolar amount of Cysteine (Cys) under the same conditions as GSH, where the reactivity of probe to thiol was ensured by the formation of **NCB** and corresponding cyclization product for Cys (**CA**) (m/z for $M+H^+$: 162.9741) (**Scheme 6.2b**). Next, we predicted that in the presence of any other thiol-sensitive reactive species, the probe would remain intact due to the plausible interaction of GSH with the thiol-reactive group. Thus, we added **NAPB** to a reaction vessel

containing an equimolar mixture of GSH and *N*-propylmaleimide (NPM), which is a popular Michael-acceptor that is extremely susceptible to reaction with thiols. To our delight, we observed the formation of an NPM-GSH conjugate **(GNA)** (m/z for $M+H^+$: 491.3078) along with the preservation of **NAPB** (m/z for $M+H^+$: 391.3051), which showcases the selective interaction of the probe to GSH (**Scheme 6.2c**). Furthermore, the selectivity of **NAPB** to biothiols was ascertained by subjecting the former to an equimolar mixture of GSH and Cys (1:1). After an hour of incubation with the GSH:Cys mixture, the LC-MS analysis affirms the formation of **GA**, but no molecular ion peak pertaining to **CA** was noted.

Scheme 6.2. Nucleophilic reactions of probe NAPB.[a]

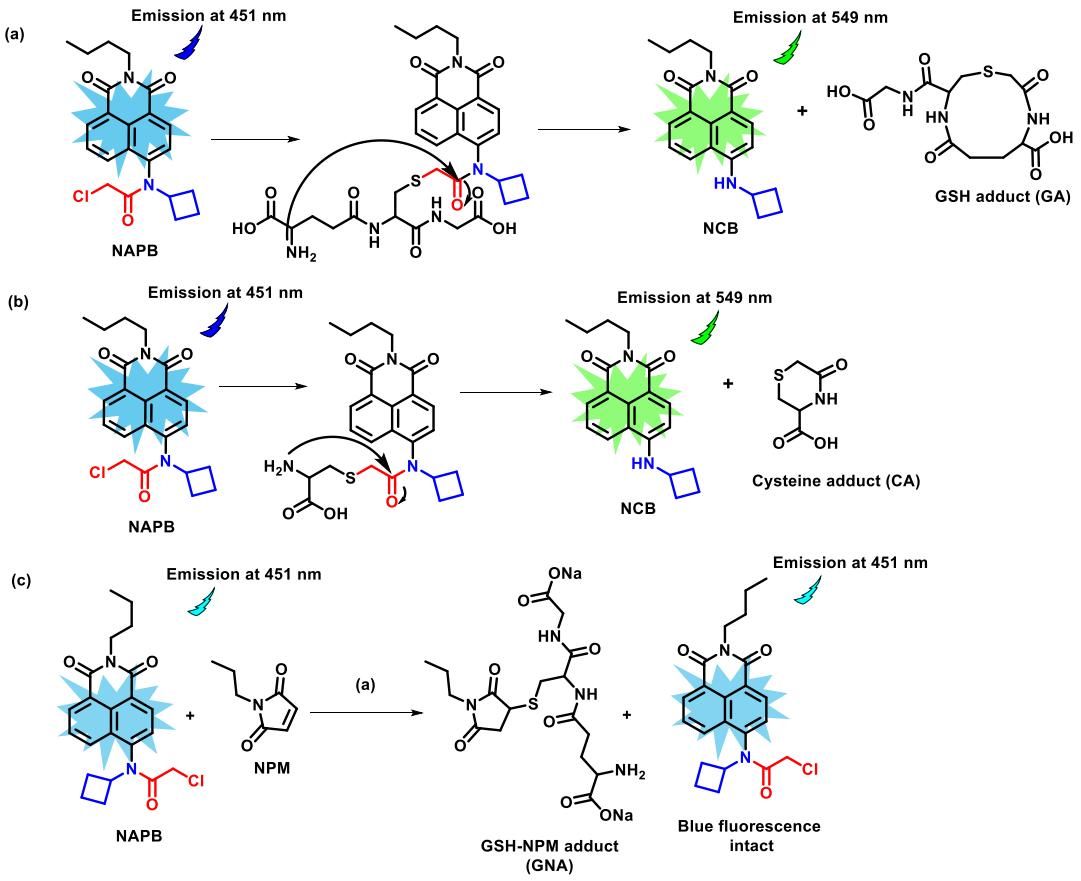

[a]**Reagents and Conditions. (a) NAPB** (0.012 mmol) in DMSO, GSH (1 equiv.) and Na_2CO_3 (cat.) in water (pH=8.5), rt, 30 mins; **(b) NAPB** (0.012 mmol) in DMSO, Cys (1 equiv.) and Na_2CO_3 (cat.) in water (pH = 8.5),

rt, 30 mins; **(c)** NPM (1 equiv.), GSH (1 equiv.), Na_2CO_3 (1.5 equiv.) in water, stirred for 10 mins, **NAPB** (0.012 mmol) in DMSO, rt, 30 mins.

6.2.3. UV- VIS characterization of probe NAPB in response to GSH

The photophysical behaviour of the probe **NAPB** (1.25 μM) was determined in phosphate buffer (mixed with DMSO in a ratio of 8:2, pH 8.5) (figure 6.2). A broad absorption band of **NAPB** was recorded with an absorbance maximum at 345 nm. Upon addition of GSH (1 equiv. dissolved in PBS), the absorption band redshifts to 445 nm from 345 nm, which can be attributed to the regeneration of the parent fluorophore **NCB**. Further, **NAPB** shows a fluorescence emission band centered at 451 nm and thus emits bright blue fluorescence when excited at 345 nm. The addition of GSH (1 equiv.) to the **NAPB** (1.25 μM) redshifts the emission band to 549 nm (corresponding to **NCB**), emitting a yellowish-green fluorescence. This creates a ratiometric response of probe **NAPB** in the presence of GSH.

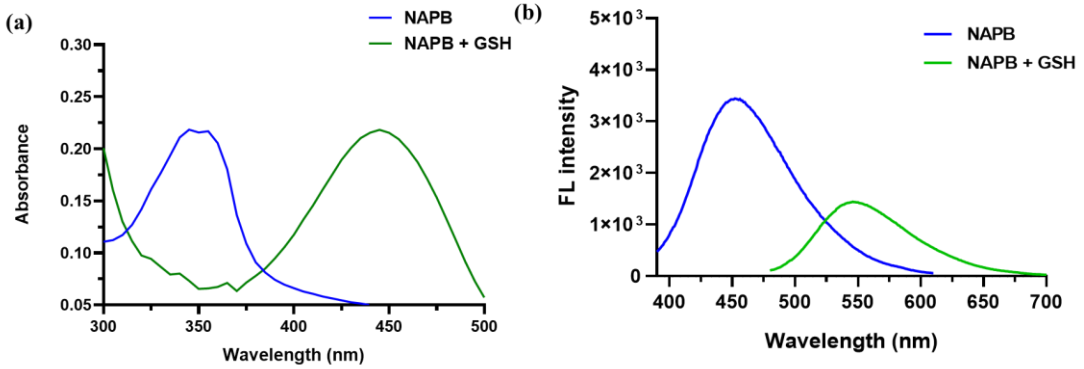

Figure 6.2. UV-VIS absorption spectra (a) and fluorescence emission spectra (b) of NAPB (in phosphate buffer mixed with DMSO in a ratio of 8:2, pH 8.5) before and after the addition of Glutathione (GSH) (1 equiv. in PBS) (λ_{ex}: 345 nm and 445 nm).

6.2.4. Concentration-based Response of NAPB towards GSH

The fluorescence titration of probe **NAPB** (1.25 μM in phosphate buffer mixed with DMSO in a ratio of 8:2, pH 8.5) with GSH solution in PBS (0-20 equiv.) was examined. As the GSH concentration increased, the fluorescence intensity of the emission band at 451 nm gradually decreased, while the emission band at 549 nm concurrently intensified. This was observed when excited at 345 nm and 445 nm, respectively (figure 6.3a-b). When the fluorescent intensities at 451 nm and 549 nm were graphed against the GSH concentration (0-20 equiv.) (figure 6.3c), a consistent decrease in the blue fluorescence emission (F_{445}) and a gradual increase in the yellowish-green fluorescence (F_{549}) were observed up to a GSH concentration of 10 equiv., after which the probe reached saturation. A linear relationship was noted between the fluorescence intensity ratio (F_{549}/F_{451}) of probe NAPB and the GSH concentration within the range of 0 - 10 equivalents ($R^2 = 0.993$). Additionally, a low detection limit of 39.1 nM was calculated using 3δ/K, where δ represents the standard deviation of blank measurements and K

represents the slope of the plot of fluorescence intensity versus the sample concentration (figure 6.3d).

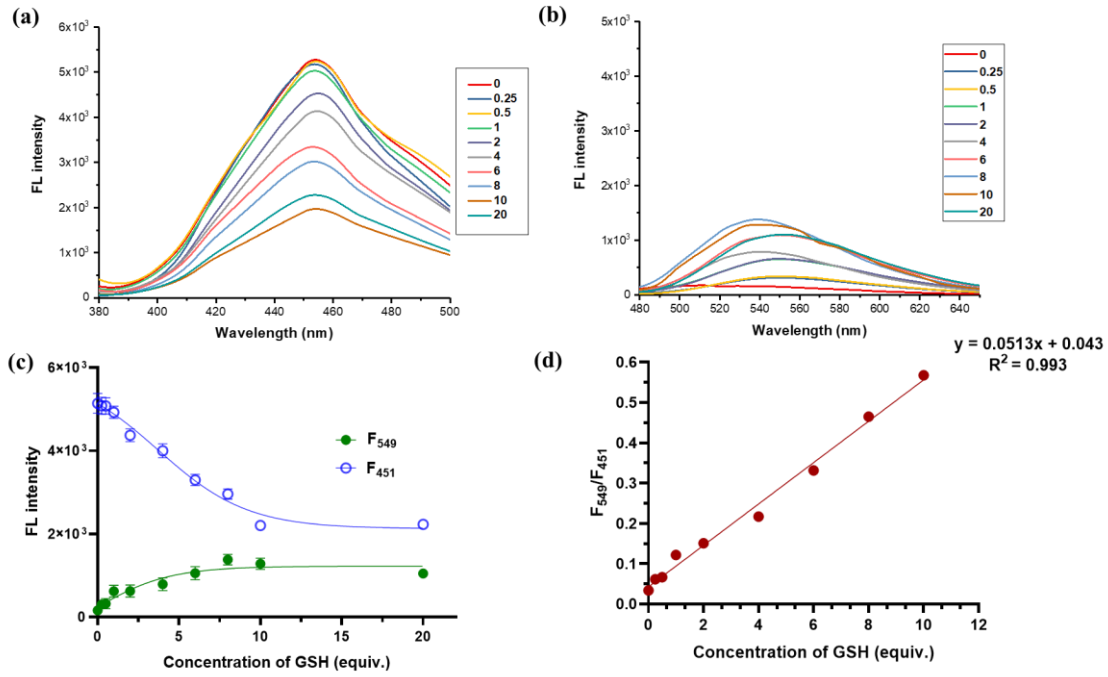

Figure 6.3. Fluorescence responses of **NAPB** (1.25 μM) to various concentrations of GSH (0 - 20 equiv.) when excited at λ_{ex} = 345 nm (a) and λ_{ex} = 445 nm (b), respectively; (c) Fluorescence intensities of **NAPB** (1.25 μM) at 451 nm and 549 nm in response to increasing concentrations of GSH (0-20 equiv.) when excited at λ_{ex} = 345 nm and λ_{ex} = 445 nm, respectively; (d) GSH concentration-based response curve of **NAPB** shows linear relationship within a concentration range of 0 -10 equiv.

6.2.5. Time-based Response to GSH and pH Stability Study of NAPB

To assess the response of probe to GSH detection over time, **NAPB** was exposed to a fixed concentration of GSH (1 equiv.) for an hour. The addition of GSH resulted in an immediate increase in fluorescence emission at 549 nm within about 5-10 minutes, which continued to intensify over time and reached equilibrium after 35 minutes (figure 6.4a). Furthermore, we

examined the stability of **NAPB** within the physiological range (pH 4-8) and were delighted to discover its excellent stability (figure 6.4b).

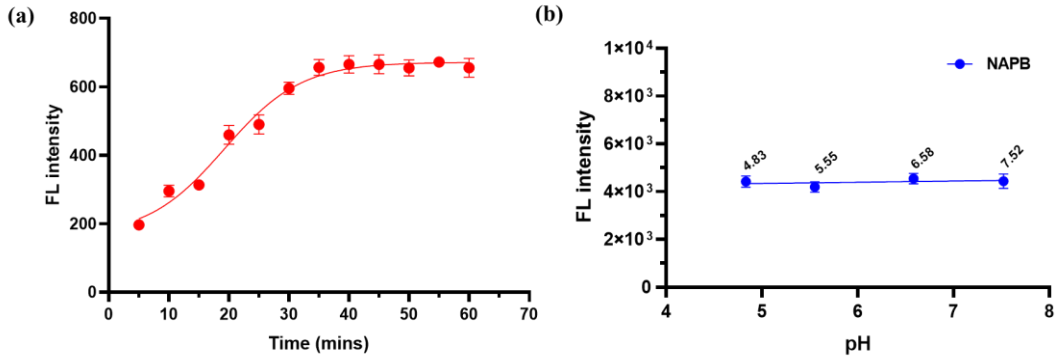

Figure 6.4. (a) Time-dependent fluorescence response of **NAPB** (1.25 μM) to GSH (1 equiv.) at 549 nm. (λ_{ex}: 445 nm); (b) Evaluation of the stability of probe **NAPB** (1.25 μM) to changes in pH (4-8) at λ_{em} = 549 nm (λ_{ex}: 445 nm).

6.2.6. Biocompatibility Assay and *In vitro* Cellular Imaging of NAPB in cancer cells

Upon evaluating the selectivity, sensitivity, and pH stability of the probe, we tested its application for detecting and imaging GSH in living cells. Utilizing the MTT assay technique, we thoroughly assessed the biocompatibility of **NAPB** in HepG2 hepatocarcinoma cell lines. Following the 24-hour incubation of HepG2 cells with NAPB in a concentration range of 1 to 10 μM, we observed a significant trend. The cell viability remained consistently above 90% at lower concentrations (1-5 μM) but decreased below 80% at 10 μM. Consequently, we confidently confirmed the safety of using the probe in living systems at a concentration of 5 μM.

To conduct fluorescence imaging of GSH in living cells using the probe (figure 6.5b), HepG2 cells were strategically incubated with **NAPB**, followed by treatment with exogenous GSH and a control compound NPM to validate the probe's selectivity to GSH. The fluorescence imaging revealed that **NAPB** (5 μM) incubated cells emitted intense blue fluorescence in the blue

channel (λ_{ex}: 357-344 nm, and λ_{em}: 447-460 nm) and weak fluorescence in the green channel (λ_{ex}: 470 nm, and λ_{em}: 510-542 nm), indicating a lower concentration of endogenous GSH.

Subsequently, when the probe-treated cells were incubated with exogenous GSH (5 μM) for 30 minutes, the green fluorescence intensity exhibited a notable surge due to the cleavage of **NAPB** to the parent fluorophore **NCB** (λ_{em}: 549 nm) in the presence of GSH. Furthermore, when HepG2 cells pre-treated with **NAPB** (5 μM) for an hour were incubated with a mixture of exogenous GSH (5 μM) and the control compound NPM (5 μM) for 30 minutes, the green channel fluorescence disappeared entirely. This unequivocally points to the removal of free GSH from the cells by interaction with NPM, leaving the probe intact, which singularly emitted at 451 nm.

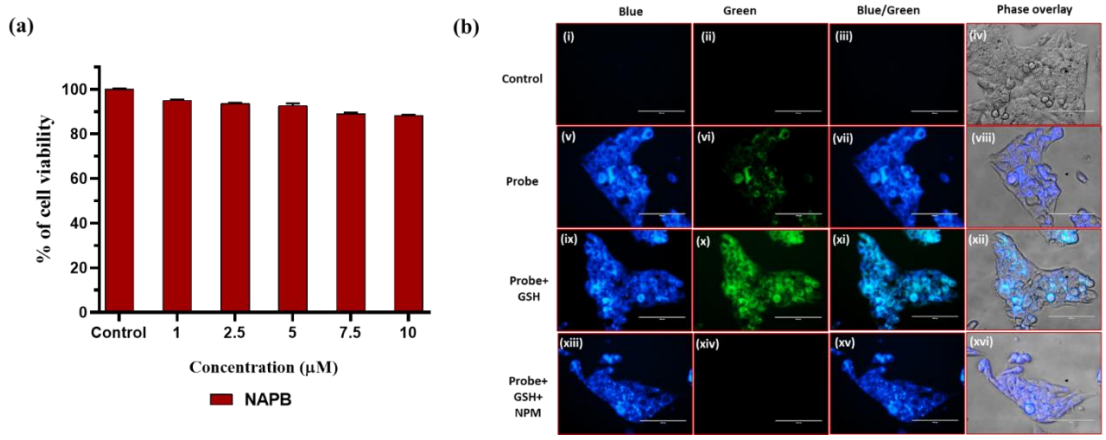

Figure 6.5. (a) Measurement of percent viability of HepG2 liver cancer cells incubated with probe **NAPB** at various concentrations ranging from 1 μM to 10 μM using MTT assay. Statistical analysis has been done by One-way ANOVA followed by Tukey's test where * denotes a significant difference ($p<0.05$); (b) Fluorescent and merged images of HepG2 cells when treated with probe NAPB in the absence and presence of exogenous GSH and NPM; (i-iv) Control, (v-viii) Cells were treated with probe **NAPB** (5 μM) only for 1h and then the image was captured, (ix-xii) Cells were treated with probe **NAPB** (5 μM) only for 1h, followed by GSH (5 μM) for 30 mins and then image was captured, (xiii-xvi) Cells were treated with probe

NAPB (5 μM) only for 1h, followed by a mixture of GSH:NPM (5 μM each) for 30 mins and then image was captured. λ_{ex}: 357-344 and 470 nm, and λ_{em}: 447-460 and 510-542 nm. Scale bar = 100 μm.

6.3. Conclusion

We have developed a novel ratiometric probe, **NAPB**, which is based on a highly efficient light-emitting fluorophore, namely cyclobutylamino-functionalized naphthalimide (**NCB**). This probe is designed for the selective and sensitive detection of GSH. **NAPB** utilizes a simple method of nucleophilic substitution followed by cyclization to detect GSH. Our control experiment with NPM confirms the selectivity of **NAPB** towards GSH. In the presence of GSH, **NAPB** exhibits a ratiometric change in fluorescence emission from blue to greenish yellow due to the cleavage of the former to its parent fluorophore **NCB**. The probe demonstrates a linear relationship with GSH concentration within a range of 0 to 10 equivalents and possesses a low detection limit of 39.1 nM. It shows a rapid response to GSH within 5-10 minutes of incubation and shows substantial pH stability within the physiological range of 4-8. MTT assay in HepG2 cells confirms its safety, as cells maintain over 90% viability up to a concentration of 5 μM. Fluorescence imaging in HepG2 cells highlights the potential of **NAPB** as a powerful tool for detecting GSH in living cells. Furthermore, the probe holds great promise for advancing research on GSH-related disease diagnosis and inspiring the development of other innovative fluorescent probes for GSH or other biothiol detection.

6.4. Experimental section

6.4.1. Materials and methods

All chemicals were purchased from TCI Chemicals and Spectrochem Ltd, and used as received. Molychem silica gel (60-120 mesh) was used for column chromatography, and thin-layer chromatography was performed on Merck pre-coated silica gel 60-F254 plates. All other

chemicals and solvents were obtained from commercial sources and purified using standard methods. The ^{1}H NMR and ^{13}C NMR spectra were recorded on Bruker-Advance 600 MHz spectrometers. Chemical shifts (δ) are reported in parts per million (ppm), using TMS (δ = 0) as an internal standard and d^6-DMSO as NMR solvent. The mass spectrum of the compounds has been obtained by Waters Q-ToF Premier Mass Spectrometer. UV absorbance was measured on Agilent Cary UV 60 UV-Visible Spectrophotometer. Fluorescence data were recorded on a Molecular Devices SpectraMax M5 multimode plate reader. Solvent used for fluorescence spectra: PBS, 1X (SRL Chemicals). GraphPad Prism ver. 7.0a (GraphPad Software, Inc.) and Origin2017 softwares were used to analyze data and generate graphs. HepG2 hepatocarcinoma cell lines were procured from the National Center for Cell Science (NCCS), Pune, India. DMEM (Dulbecco's Modified Eagle Medium) was chosen as the cell culture medium, and was purchased along with 12 well cell culture plate from Genetics (Genetics Biotech Asia Pvt. Ltd). The T-25 flasks and 96 well plates were purchased from Eppendorf. Other growth media essentials, such as Streptomycin, Penicillin, Trypsin-EDTA, and Fetal Bovine Serum (FBS) were purchased from Gibco. Phosphate Buffer Saline (PBS) was prepared using high grade analytical chemicals. The cells were cultured in FBS and penicillin-streptomycin supplemented DMEM and grown in a humidified CO_2 incubator at 37 ^{o}C.

6.4.2. Step-wise synthesis of probe NAPB

6.4.2.1. Procedure of synthesis of precursor B.

A 10 ml round bottomed flask was charged with 6-bromo-1*H*,3*H*-benzo[de]isochromene-1,3-dione (**A,** 0.825 g, 3 mmol) and *n*-butylamine (2.5 equiv.) in ethanol (5 mL) as solvent and refluxed at 80 ^{o}C for 2 h. After cooling the reaction mixture to ambient temperature, the solvent was evaporated *in vacuo* and the crude mixture was then diluted with water (10 mL) and extracted with ethyl acetate (15 mL ×3). After drying with anhydrous Na_2SO_4, the organic

phase was evaporated to dryness and purified by column chromatography using 15% ethyl acetate: hexane as eluent to yield **B** (75% yield) as a white solid.

6.4.2.2. Procedure of synthesis of NCB.

Compound **B** (0.3 mmol, 1 equiv.) and cyclobutylamine (1.5 equiv.) were weighed and placed in a 25 ml round bottomed flask containing 2 mL of DMSO. To this mixture triethylamine (1.5 equiv.) was added as a base and the reaction mixture was stirred at 110 ºC for 6 h. After cooling the reaction mixture to ambient temperature, the crude mixture was then diluted with water (10 mL) and extracted with ethyl acetate (10 mL ×3). After drying with anhydrous Na_2SO_4, the organic phase was evaporated to dryness and purified by column chromatography using 15% ethyl acetate: hexane as eluent to yield **NCB** as a yellow crystalline solid (78% yield).

6.4.2.3. Procedure of synthesis of NAPB.

NCB (0.5 mmol) and dried Na_2CO_3 (2 equiv.) were taken in ACN (1.5 mL) as solvent in a 25 mL reaction flask and stirred at 0ºC on an ice bath. To the slurry, a solution of chloroacetyl chloride (5 eq.) in 1.5 mL of ACN was added dropwise and the reaction mixture was then refluxed at 80 ºC for 2h. As soon as the yellow fluorescence of **NCB** disappeared, the reaction mixture was brought to room temperature and diluted with water (25 mL) and extracted with ethyl acetate (10 mL ×3). After drying with anhydrous Na_2SO_4, the organic phase was evaporated to dryness and purified by column chromatography using 18% ethyl acetate: hexane as eluent to yield **NAPB** as a yellow liquid (76% yield).

6.4.3. Reaction of NAPB with biothiols (GSH and Cys).

A 5 mL glass vial charged with **NAPB** (0.012 mmol) dissolved in DMSO (100 μL) was stirred with dropwise addition of biothiols (GSH and Cys) (1 equiv.) and catalytic amount of dried Na_2CO_3 (to maintain pH at 8.5) dissolved in water (100 μL) at ambient temperature and open-air conditions for 30 mins. The pH of the reaction mixture was monitored at regular intervals

with pH paper. The selectivity experiment was carried out using an equimolar mixture (1:1) of GSH:Cys in water in place of GSH/Cys in the above mentioned reaction protocol and the reaction was carried out for 1 h.

6.4.4. Control experiment with *N*-Propylmaleimide (NPM).

In a glass vial (5 mL), NPM (1 equiv.), GSH (1 equiv.) and dried Na_2CO_3 (1.5 equiv.) were added in sequence and dissolved in water (100 μL) with continuous stirring at room temperature. After 10 mins, **NAPB** (0.012 mmol) dissolved in DMSO (100 μL) was added to the reaction mixture and stirred at ambient temperature and open-air conditions for another 30 mins.

6.4.5. UV-VIS and fluorescence measurements of probe NAPB.

The stock solution of probe **NAPB** (100 μM) was made in 25 mM PBS mixed with DMSO in a ratio of 8:2 (pH 7.4). It was then diluted to 1.25 μM concentration using PBS and used freshly. The stock solutions of GSH (100 μM) and Cys (100 μM) were prepared in PBS and then diluted to serial concentrations ranging between 0-20 equivalents w.r.t. **NAPB** (1.25 μM) and used freshly. The absorption and emission wavelengths of the resultant solution of the probe were measured in the absence and in the presence of GSH in PBS (1 equiv.) and plotted into graphs. For pH stability study, the buffers having pH ranges 4-8 were prepared using deionized water following standard protocol and freshly used. Probe **NAPB** (20 μM) was placed in each buffer system and incubated for 30 mins at 37 ºC before measuring the fluorescence intensities.

6.4.6. *In vitro* cytotoxicity testing of NAPB using MTT assay.

Cytotoxicity of probe **NAPB** against HepG2 cell lines was analyzed in a 96-well cell culture plate, which contained 1×10^4 cells/well. The cells were distributed such that each well contained 100 μL of the complete culture medium. The culture plate was then placed in a CO_2

incubator with 5% CO_2 at 37°C for 24 h to allow cell adherence. After 24 h of incubation, the media was aspirated, and fresh media was added comprising of probe **NAPB** at different concentrations within a range of 1 - 10 μM and incubated for another 24 h. After 24 h, media was aspirated, and fresh media containing of MTT (3-(4,5-dimethylthiazol-2-yl)-2,5-diphenyltetrazolium bromide) was added to each well and incubated for an additional 2h at 37°C. The MTT-containing media was then aspirated, and 100 μL of DMSO was added to each well and subsequently incubated for another 30 mins to dissolve the formazan precipitate. The plate was incubated for the next 10 mins with gentle shaking. The optical density of each well was measured at 570 nm using a microplate reader.

6.4.7. Fluorescence imaging of NAPB-treated HepG2 cells.

Hep G2 cells were seeded in a 12-well culture plate at 3 x 10^4 cells/well density and incubated overnight in a CO_2 incubator with 5% CO_2 at 37°C to obtain cell adherence. After 24 h of incubation, the media was aspirated, and fresh media was added containing 5 μM **NAPB** for 1 h. Next, probe-treated cells in four of these wells were incubated with GSH (5 μM) and the other four were incubated with a GSH:NPM mixture (5 μM each) for another 30 mins. After completion of treatment, cells were washed with cold PBS three times, and images were captured using an inverted fluorescence microscope in the blue channel (λ_{abs}: 357/44 nm and λ_{em}: 447/60 nm) at 400 X magnification.

6.4.8. Spectral data of NAPB

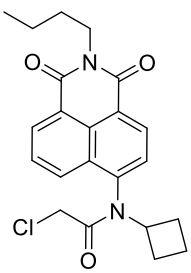

***N*-(2-butyl-1,3-dioxo-2,3-dihydro-1H-benzo[de]isoquinolin-6-yl)-2-chloro-N-cyclobutylacetamide (NAPB).** The molecule was synthesized following the step-wise protocol mentioned above. The compound was purified by column chromatography using 18% ethyl acetate:hexane. The probe **NAPB** was obtained as yellow liquid with 76 % yield. ^{1}H NMR (600 MHz, d^6-DMSO) δ 8.58 - 8.53 (m, 2H), 8.27 - 8.21 (m, 1H), 7.95 (t, J = 7.8 Hz, 1H), 7.90 (d, J = 7.2 Hz, 1H), 5.07 (quint, J = 9.0 Hz, 1H), 4.07 (t, J = 7.2 Hz, 2H), 3.92 (d, J = 13.8 Hz, 1H), 3.66 (d, J = 13.8 Hz, 1H), 2.27 – 2.19 (m, 2H), 1.93 – 1.83 (m, 2H), 1.63 (quint, J = 7.8 Hz, 2H), 1.42 – 1.34 (m, 4H), 0.93 (t, J = 7.2 Hz, 3H). ^{13}C NMR (150 MHz, d^6-DMSO) δ 165.5, 163.7, 163.3, 140.2, 131.7, 131.2, 130.1, 129.8, 129.0, 123.4, 123.26, 52.2, 43.4, 30.0, 29.2, 28.1, 20.2, 15.0, 14.1. HRMS (ESI) m/z calculated for $C_{20}H_{19}O_3N_2Cl$ [M + H]$^+$ calculated as 399.1470 and 401.1440, found 399.1681 and 401.1819.

6.5. References

(1) Calabrese, G.; Morgan, B.; Riemer, J. Mitochondrial Glutathione: Regulation and Functions. *Antioxid. Redox Signal.* **2017**, *27* (15), 1162–1177. https://doi.org/10.1089/ars.2017.7121.

(2) Forman, H. J.; Zhang, H.; Rinna, A. Glutathione: Overview of Its Protective Roles, Measurement, and Biosynthesis. *Mol. Aspects Med.* **2009**, *30* (1), 1–12. https://doi.org/10.1016/j.mam.2008.08.006.

(3) Sies, H. Glutathione and Its Role in Cellular Functions. *Free Radical Biol. Med.* **1999**, *27* (9), 916–921. https://doi.org/10.1016/S0891-5849(99)00177-X.

(4) Kim, S. J.; Kim, H. S.; Seo, Y. R. Understanding of ROS-Inducing Strategy in Anticancer Therapy. *Oxid Med Cell Longev* **2019**, *2019*, 5381692. https://doi.org/10.1155/2019/5381692.

(5) Jones, D. P. [11] Redox Potential of GSH/GSSG Couple: Assay and Biological Significance. In *Methods in Enzymology*; Sies, H., Packer, L., Eds.; Protein Sensors and Reactive Oxygen Species - Part B: Thiol Enzymes and Proteins; Academic Press, 2002; Vol. 348, pp 93–112. https://doi.org/10.1016/S0076-6879(02)48630-2.

(6) Giblin, F. J. Glutathione: A Vital Lens Antioxidant. *J. Ocul. Pharmacol. Ther.* **2000**, *16* (2), 121–135. https://doi.org/10.1089/jop.2000.16.121.

(7) Tian, X.; Kumawat, L. K.; Bull, S. D.; Elmes, R. B. P.; Wu, L.; James, T. D. Coumarin-Based Fluorescent Probe for the Detection of Glutathione and Nitroreductase. *Tetrahedron* **2021**, *82*, 131890. https://doi.org/10.1016/j.tet.2020.131890.

(8) Wu, L.; Tian, X.; Groleau, R. R.; Wang, J.; Han, H.-H.; Reeksting, S. B.; Sedgwick, A. C.; He, X.-P.; Bull, S. D.; James, T. D. Coumarin-Based Fluorescent Probe for the Rapid Detection of Peroxynitrite 'AND' Biological Thiols. *RSC Adv 10* (23), 13496–13499. https://doi.org/10.1039/d0ra02234a.

(9) Das, S.; Indurthi, H. K.; Asati, P.; Saha, P.; Sharma, D. K. Benzothiazole Based Fluorescent Probes for the Detection of Biomolecules, Physiological Conditions, and Ions Responsible for Diseases. *Dyes Pigm.* **2022**, *199*, 110074. https://doi.org/10.1016/j.dyepig.2021.110074.

(10) Cao, Y.; Liu, X.; Zhang, J.; Liu, Z.; Fu, Y.; Zhang, D.; Zheng, M.; Zhang, H.; Xu, M.-H. Design of a Coumarin-Based Fluorescent Probe for Efficient *In Vivo* Imaging of Amyloid-β Plaques. *ACS Chem. Neurosci.* **2023**, *14* (5), 829–838. https://doi.org/10.1021/acschemneuro.2c00468.

(11) Cao, M.; Chen, H.; Chen, D.; Xu, Z.; Liu, S. H.; Chen, X.; Yin, J. Naphthalimide-Based Fluorescent Probe for Selectively and Specifically Detecting Glutathione in the Lysosomes of Living Cells. *Chem. Commun.* **2015**, *52* (4), 721–724. https://doi.org/10.1039/C5CC08328A.

(12) Das, S.; Goswami, P.; Verma, V. K.; Indurthi, H. K.; Kumar, M.; Koch, B.; Sharma, D. K. Rapid Access to 7-Substituted Cycloalkylamino and Alkylamino Analogues of 4-Methylcoumarin Reveals Surprising Emitters. *Dyes Pigm.* **2023**, *217*, 111407. https://doi.org/10.1016/j.dyepig.2023.111407.

(13) Li, H.; Yang, Y.; Qi, X.; Zhou, X.; Ren, W. X.; Deng, M.; Wu, J.; Lü, M.; Liang, S.; Teichmann, A. T. Design and Applications of a Novel Fluorescent Probe for Detecting Glutathione in Biological Samples. *Anal. Chim. Acta* **2020**, *1117*, 18–24. https://doi.org/10.1016/j.aca.2020.03.040.

(14) Qi, X.; Shang, L.; Liang, S.; Li, H.; Chen, J.; Xin, C.; Zhao, J.; Deng, M.; Wang, Q.; He, Q.; Lv, M.; Teichmann, A. T.; Wang, Z.; Yang, Y. Development and Applications of a Coumarin-Based "Turn-on" Fluorescent Probe for Effectively Discriminating Reduced Glutathione from Homocysteine and Cysteine in Living Cells and Organisms. *Dyes Pigm.* **2021**, *194*, 109625. https://doi.org/10.1016/j.dyepig.2021.109625.